Characterization and Application of Nanomaterials 2025, 8(1), 10286.
https://doi.org/10.24294/can10286

Article

Comparative analysis of zinc precursors in the hydrothermal synthesis of zinc oxide hollow spheres

Omid Khanali, Khanali Nekouee*, Hamed Naderi-Samani

Faculty of Materials and Manufacturing Technologies, Malek Ashtar University of Technology, Tehran 1491912354, Iran
*** Corresponding author:** Khanali Nekouee, khnekouee@gmail.com

CITATION

Khanali O, Nekouee K, Naderi-Samani H. Comparative analysis of zinc precursors in the hydrothermal synthesis of zinc oxide hollow spheres. Characterization and Application of Nanomaterials. 2025; 8(1): 10286. https://doi.org/10.24294/can10286

ARTICLE INFO

Received: 13 November 2024
Accepted: 13 December 2024
Available online: 17 February 2025

Abstract: Zinc oxide (ZnO) hollow spheres are gaining attention due to their exceptional properties and potential applications in various fields. This study investigates the impact of different zinc precursors Zinc Chloride ($ZnCl_2$), Zinc Nitrate [$Zn(NO_3)_2$], and Zinc Acetate [$Zn(CH_3COO)_2$] on the hydrothermal synthesis of ZnO hollow spheres. A comprehensive set of characterization techniques, including Field Emission Scanning Electron Microscopy (FE-SEM), X-ray Diffraction (XRD), Thermogravimetric analysis (TGA), and Brunauer-Emmett-Teller (BET) analysis, was utilized to assess the structural and morphological features of the synthesized materials. Our findings demonstrate that all samples exhibit a high degree of crystallinity with a wurtzite structure, and crystallite sizes range between 34 to 91 nm. Among the different precursors, ZnO derived from Zinc Nitrate showed markedly higher porosity and a well-defined mesoporous structure than those obtained from Zinc Acetate and Zinc Chloride. This research underscores the significance of precursor selection in optimizing the properties of ZnO hollow spheres, ultimately contributing to advancements in the design and application of ZnO-based nanomaterials.

Keywords: zinc oxide; hollow spheres; hydrothermal synthesis; precursors; morphology

1. Introduction

Zinc oxide (ZnO) stands out as a versatile material with applications in diverse fields like photocatalysis and sensors due to its unique properties [1]. Among various ZnO nanostructures, hollow spheres hold particular promise for these applications. Their high surface area, tunable pore structure, and enhanced light harvesting capabilities make them ideal candidates [2,3].

The hydrothermal method offers a simple and cost-effective approach for synthesizing ZnO hollow spheres with controlled morphologies [4]. However, a crucial factor influencing the final product is the choice of Zinc precursor. The precursor significantly impacts the formation process, ultimately affecting the structure and properties of the resulting ZnO hollow spheres [5]. Despite extensive research on ZnO nanostructures, a systematic understanding of how different precursors influence the synthesis of ZnO hollow spheres via hydrothermal methods remains limited. While the relationship between morphology and performance is established, the precise mechanisms governing ZnO nanostructure growth and their correlation with morphology require further investigation, particularly for hydrothermal synthesis using different precursors [6]. To investigate this further, our research explores the effects of various zinc precursors (Acetate, Chloride, and Nitrate) on the structural and morphological characteristics of hydrothermally synthesized zinc oxide hollow spheres. By elucidating the role of precursors, we aim

to contribute to the advancement of ZnO-based nanomaterial design and its targeted application development [7,8].

2. Experimental section

2.1. Materials

All solvents and reagents were used as received from commercial suppliers without any further purification. Zinc Nitrate anhydrous ($Zn(NO_3)_2$, 99.99% purity, (Mr = 189.36 g/mol) Sigma Aldrich), Zinc Acetate anhydrous ($ZnAc_2$, $Zn(C_2H_3O_2)_2$, 99.98%, (Mr = 183.48 g/mol), Sigma Aldrich), Zinc Chloride ($ZnCl_2$, > 99%, (Mr = 136.28 g/mol) Alfa Aesar, Germany), D-Glucose ($C_6H_{12}O_6$, 99.95% Sigma Aldrich), ethanol (EtOH, 100%, Molar Chemicals, Hungary) and Ultrapure water was used to prepare aqueous solutions for the chemical synthesis and all the experiments.

2.2. Synthesis of ZnO hollow spheres

This study employed a hydrothermal method to synthesize ZnO hollow spheres using various Zinc precursors. Zinc Chloride (ZC), Zinc Nitrate (ZN), and Zinc Acetate (ZA) served as the Zinc source, while glucose ($C_6H_{12}O_6 \cdot H_2O$, 99.5%) acted as the carbonaceous source. **Table 1** details the specific quantities of materials used for each precursor combination [9]. The ratio of Zinc precursors to glucose was considered as 1/2. A typical synthesis involved dissolving a specified amount of the chosen zinc precursor in deionized water under stirring to create a clear solution. Subsequently, glucose was introduced dropwise to initiate the hydrothermal reaction. The synthesized mixture was subsequently transferred to a 100 mL Teflon-lined stainless-steel autoclave and heated in a muffle furnace at 180 ℃ for 20 h. Upon cooling to ambient temperature, the product was collected. The resulting black precipitate was subjected to a thorough washing process using both distilled water and ethanol. Following synthesis, the black precipitate was dried in a vacuum oven at 80 ℃ for 5 h and finally calcined at 550 ℃ for 2 h. The detailed steps for preparing the ZnO hollow spheres are illustrated in the scheme of **Figure 1** [5,10,11].

Table 1. Raw materials and conditions for the hydrothermal synthesis of ZnO nanostructures.

Code of material	Chemical formula	Zinc salt Precursors	D-glucose	deionized water
ZC (Zinc Chloride)	$ZnCl_2$	0.1 mol (13.62 g)	40 g (0.2 mol)	60
ZN (Zinc Nitrate)	$Zn(NO_3)_2$	0.1 mol (18.94 g)	40 g (0.2 mol)	60
ZA (Zinc Acetate)	$Zn(CH_3CO_2)_2$	0.1 mol (18.34 g)	40 g (0.2 mol)	60

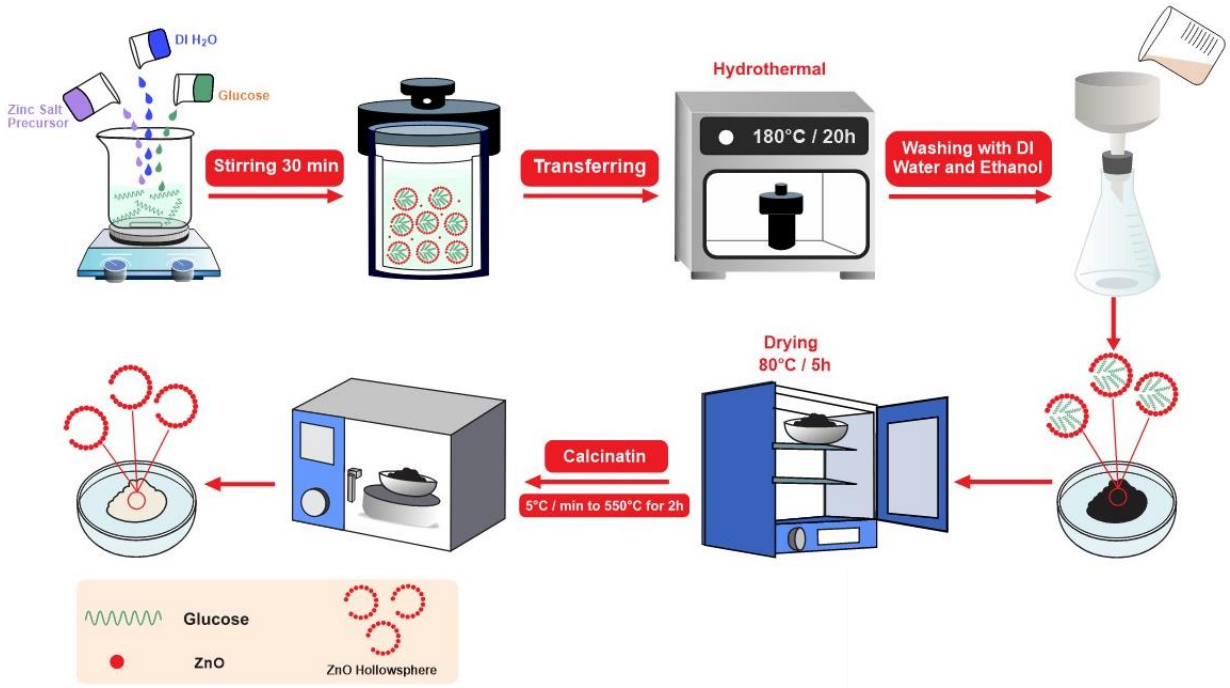

Figure 1. Schematic of progresses for the preparation of hollow sphere ZnO.

2.3. Characterization

The crystalline phases of the synthesized ZnO hollow spheres were identified using X-ray diffraction (XRD) analysis with Fe-Kα radiation source (λ = 0.1937 nm) operated at 40 kV and 150 mA at a scanning step of 0.05 in the 2Θ range 20–80_. The surface morphology and sizes of the hollow ZnO microspheres were observed by field-emission scanning electron microscopy (FE-SEM, MIRA3TESCAN-XMU with an accelerating voltage of 20 kV) with energy-dispersive spectra. This technique provides high-resolution images, allowing for detailed observation of the surface features and particle size distribution of the ZnO hollow spheres. To understand the thermal decomposition behavior and crystallization process of the as-prepared powders, thermogravimetric analysis (TGA) and differential thermogravimetric analysis (DTG) were performed using a thermogravimetric analyzer (SDT 2960, TA Instruments, New Castle, DE) under atmospheric air. The analysis was conducted over a temperature range of 40 to 600 ℃ with a heating rate of 10 ℃/min. Typically, a sample weight 10 mg was used for the tests to ensure measurable changes, while the analysis utilized ceramic crucibles due to their high-temperature stability and inertness. This technique provides information about the weight loss associated with the decomposition of organic residues and the formation of the final ZnO phase.

Functional groups present in the ZnO hollow spheres were identified through Fourier transform infrared (FT-IR) spectroscopy Jasco Model 4100_Japan FT-IR spectra of ZnO . was recorded between 400 and 4000 cm^{-1} using a resolution of 4 cm^{-1}. This technique provides valuable information about the chemical composition and bonding environment within the material.

Finally, the pore size distribution and specific surface area of the synthesized ZnO hollow spheres were determined using nitrogen gas adsorption-desorption isotherms measured with a Micromeritics ASAP 2020 Brunauer-Emmett-Teller (BET)

surface area analyzer. This analysis enables the characterization of the material's porosity, a crucial factor in various applications such as catalysis and adsorption.

3. Results and discussion

3.1. FT-IR spectroscopy

FT-IR spectroscopy was employed in the range of 400–4000 cm^{-1} to investigate the presence of organic residues and their influence on the properties of the ZnO hollow spheres. **Figure 2** presents the FT-IR spectra of samples prepared using different precursors (ZC, ZN, ZA) and calcined at 550 ℃. The broad peak observed between 3250 and 3650 cm^{-1} in all samples is attributed to the O–H stretching vibration of adsorbed water molecules on the surface of the ZnO hollow spheres. These peaks indicate the presence of surface hydroxyl groups and adsorbed water molecules, which are commonly observed in metal oxide materials. Additionally, the peak at around 1650 cm^{-1} can be assigned to the bending vibration of CO-O bonds. The characteristic peaks for ZnO are observed at 400 cm^{-1} and 570 cm^{-1}. These strong absorption bands correspond to the stretching vibrations of the Zn-O bond in the wurtzite hexagonal structure of ZnO. The presence of these peaks confirms the successful formation of the ZnO phase in the synthesized hollow spheres [10].

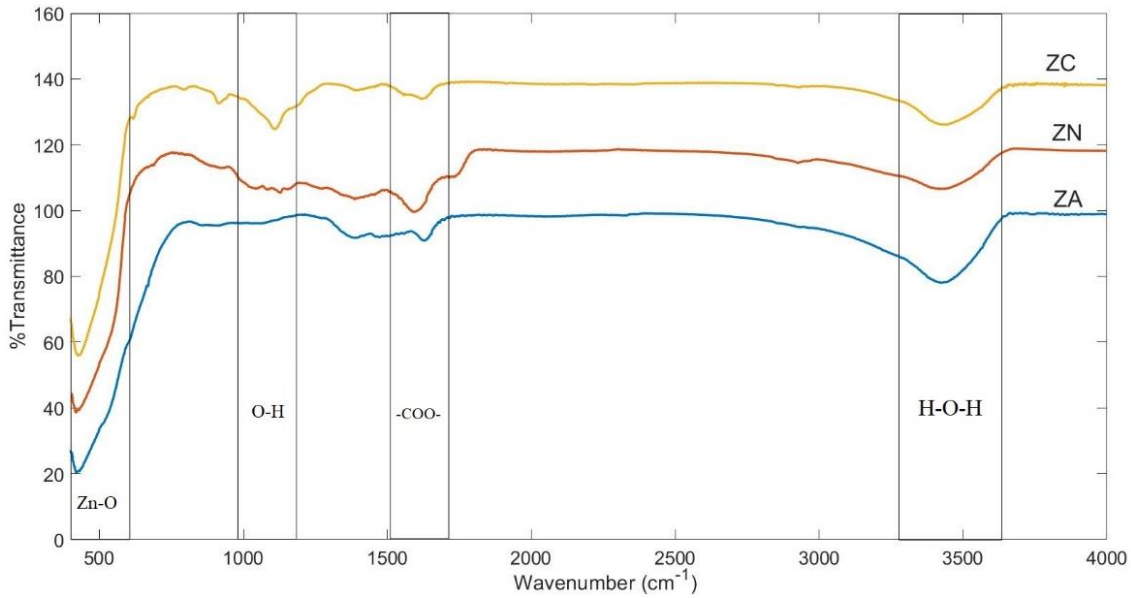

Figure 2. FT-IR spectra of ZnO hollow spheres synthesis with different precursors.

3.2. X-ray diffraction (XRD)

The crystal structures of the synthesized ZnO hollow spheres were investigated using X-ray diffraction (XRD) analysis. **Figure 3** presents the XRD patterns of the samples prepared using different precursors (ZC, ZN, ZA).

These sharp diffraction peaks, in good agreement with the standard ZnO reference pattern, indicate the high purity and good crystallinity of the ZnO phase in all samples. All samples exhibited diffraction peaks at 40°, 43°, 45°, 61°, 74°, 82°, 89° and 91°, which can be readily indexed to the (100), (002), (101), (102), (110), (103),

and (112) crystal planes of the hexagonal wurtzite structure of ZnO (Reference code: 01-076-0704) [12].

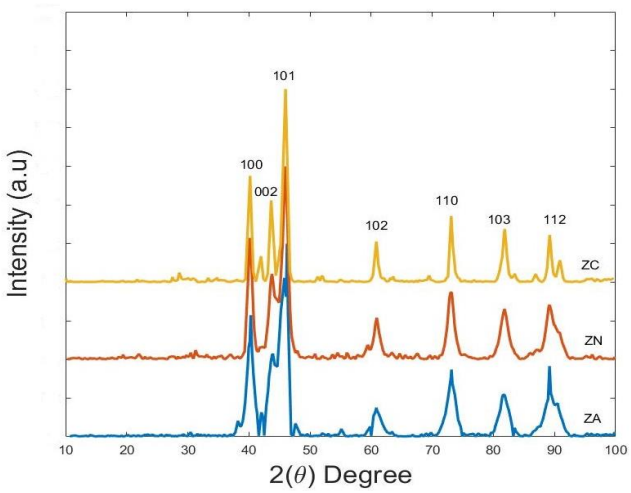

Figure 3. XRD pattern of the ZnO thin film prepared by different precursor materials.

The crystallite size of the ZnO hollow spheres was estimated using Scherrer's equation. Based on the full width at half maximum (FWHM) of the (101) peak in the XRD patterns. The calculated crystallite sizes are summarized in **Table 2**. The results indicate that the choice of precursor influences the crystallite size of the ZnO hollow spheres, with values ranging from 39 to 91 nm [13].

Table 2. Crystal size, lattice parameters of the samples with different precursors.

Zinc precursors	Pos. [°2Th.]	FWHM Left [°2Th.]	Crystallite size (nm)	Lattice parameter		c/a
				a	c	
Zinc Chloride (ZC)	46.051450	0.669120	48	3.2660	5.1988	1.5917
Zinc Nitrate (ZN)	45.820390	0.944640	34	3.2562	5.1969	1.5960
Zinc Acetate (ZA)	45.986160	0.354240	91	3.2548	5.2139	1.6019

Furthermore, the lattice parameters (a, c) and the c/a ratio were determined for each sample and are presented in **Table 2,** further confirming the successful formation of the desired crystalline phase [14].

3.3. Thermal behavior

The thermal decomposition behavior of the ZnO precursor powders (ZC, ZN, and ZA) was investigated using thermogravimetric analysis (TGA) and differential thermogravimetric analysis (DTG). These analyses were employed to determine the material's thermal stability and guide the selection of the calcination temperature. **Figure 4** presents the TG and DTG curves for the different precursors. The TG curve indicates a gradual weight loss for all samples in the temperature range of 40–600 °C. The residual weight percentages at 600 °C were approximately, 20%, 20%, and 38% for Zinc Chloride, Zinc Nitrate, and Zinc Acetate, respectively. The quantitative reduction in mass during decomposition is presented in **Table 3** [15]. The high

percentage of precipitation of zinc oxide particles in the Zinc Acetate precursor is related to the growth of irregularly shaped crystals that did not form a hallow sphere and grew as a single crystal. Also, in the FE-SEM images of **Figure 5**, these particles can be identified as See clearly.

Table 3. Thermal analysis corresponding to the TGA, TG and DTG curves.

Zinc precursors	Exothermic region (℃)	Maximum Temperature Peak (℃)	Weight loss %
Zinc Chloride (ZC)	200–460	458	80
Zinc Nitrate (ZN)	200–450	436	80
Zinc Acetate (ZA)	200–440	413	65

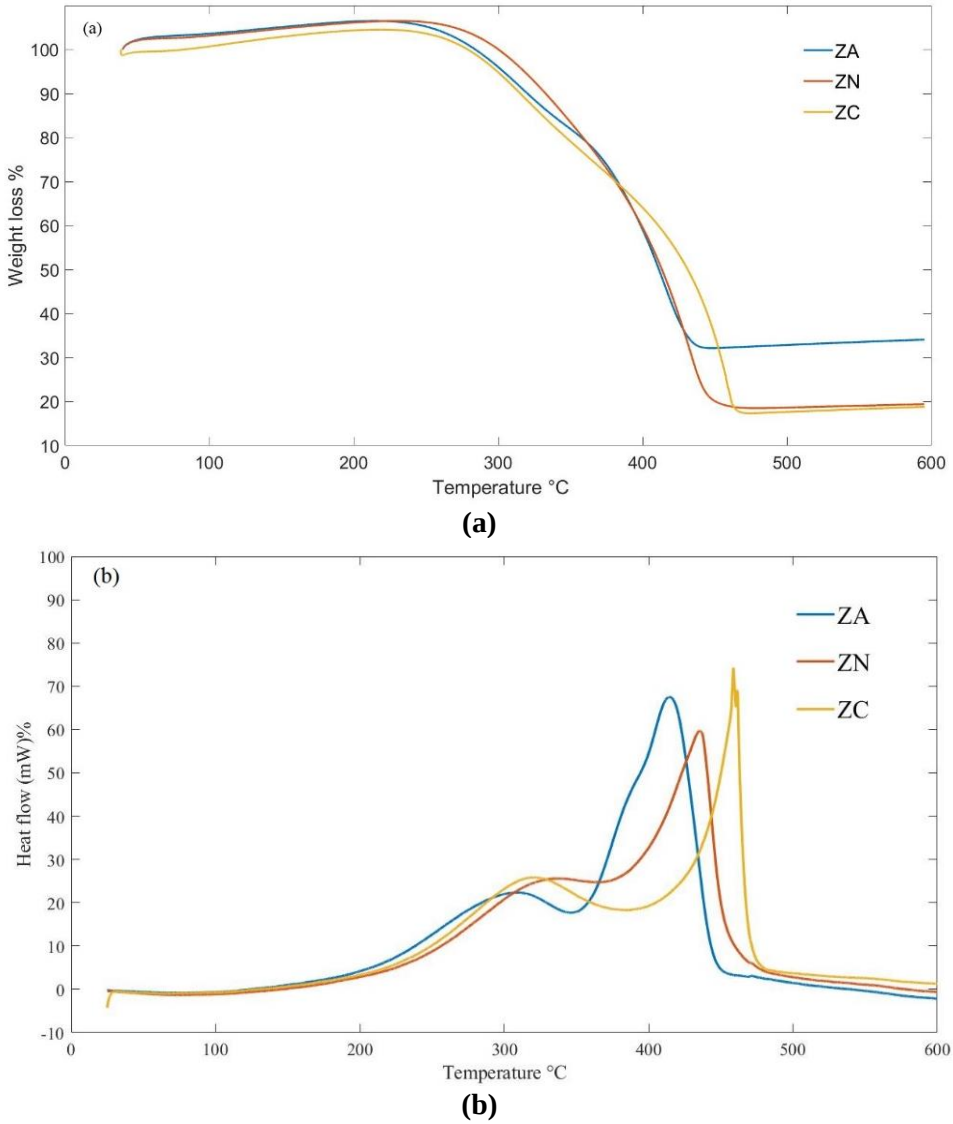

Figure 4. (a) TG; **(b)** DTG analysis of ZnO hollow sphere that synthesis by different precursors.

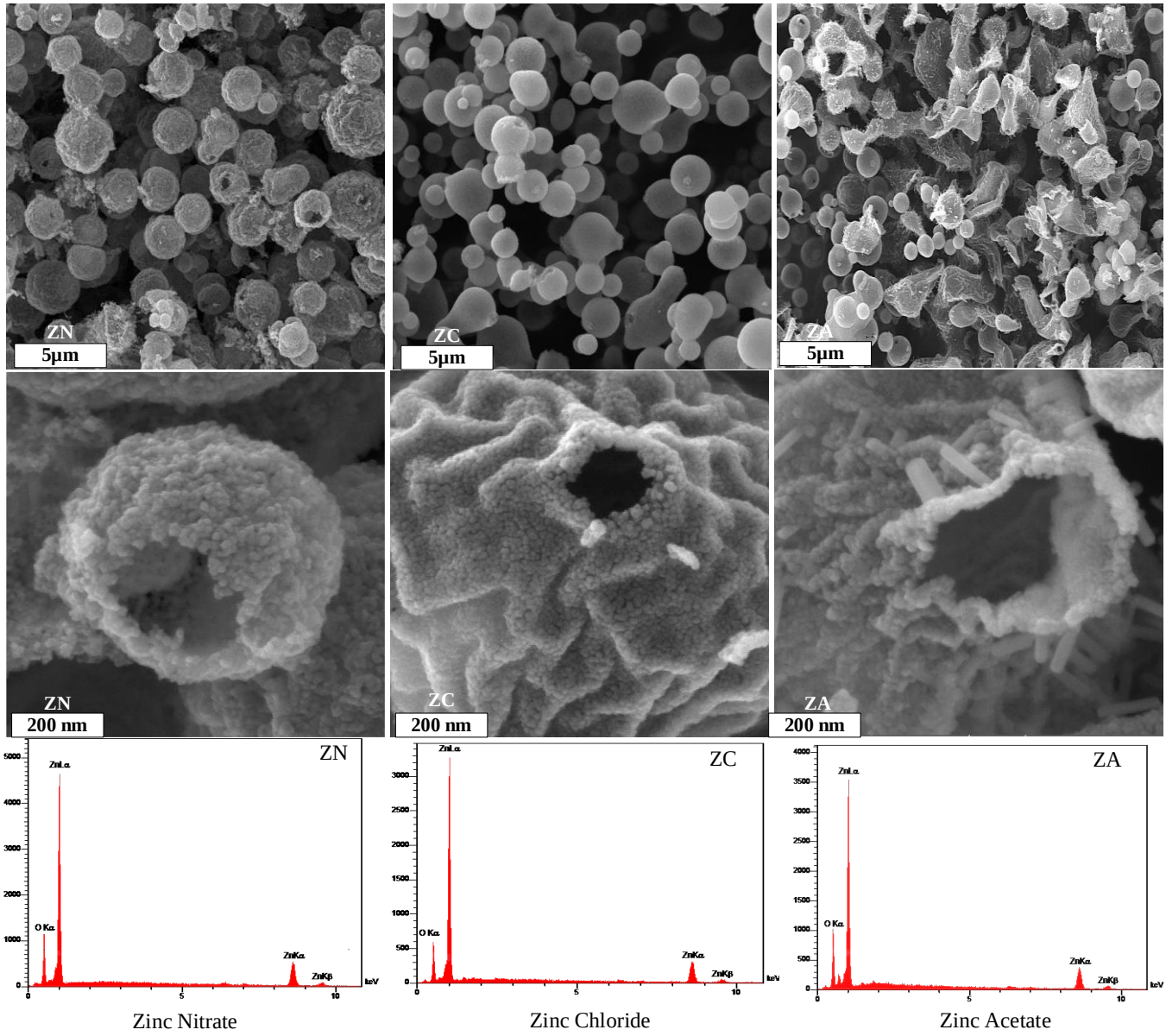

Figure 5. FE-SEM and EDS images of ZnO hollow sphere that synthesis by different precursors.

Two prominent peaks are observed in the DTG curves, located around 300 ℃ and 440 ℃. The first peak can be attributed to the desorption of water molecules physically adsorbed on the precursor surfaces. The second, more significant peak at around 440 ℃ corresponds to the decomposition of residual carbon species that might be physically or chemically bound to the precursor materials.

A significant weight loss is observed in the temperature range of 320–460 ℃, coinciding with the DTG peak at 440 ℃. This suggests the decomposition of organic moieties present in the precursors. The TG curve plateaus above 460 ℃, indicating minimal further weight loss. This implies that at this temperature, the residual organic components from the precursors are nearly completely decomposed.

These findings suggest that a calcination temperature above 460 ℃ is necessary to ensure the complete removal of organic residues and achieve the desired final product composition [16].

3.4. Morphological analysis

Figure 5 shows FE-SEM images of distinct morphologies of ZnO hollow spheres synthesized using different precursors. ZnO samples derived from Zinc Chloride and Zinc Nitrate exhibited well-defined hollow spherical structures with smooth surfaces. In contrast, ZnO synthesized from Zinc Acetate displayed irregular morphologies with partial aggregation and the presence of smaller nanoparticles. Also, we can see nanoparticles that have not turned into hallow spheres and they have grown in the form of rods. This has led to the amount of weight percentage produced in Zinc Acetate precursor being higher than others. It can also be seen in **Figure 5** that the diameter of ZnO hallow spheres synthesized for Zinc Nitrate precursor is in the range of 500 nm, while the diameter of hallow spheres synthesized for Zinc Chloride and Zinc Acetate precursors is in the range of 700 nm. EDS analysis for all three types of precursors shows that Zinc oxide is well synthesized and does not contain any impurities.

3.5. Surface properties

The specific surface area, pore size distribution, and specific pore volume of the calcined ZnO hollow spheres prepared from different precursors were determined using nitrogen adsorption-desorption isotherms measured with a Brunauer-Emmett-Teller (BET) surface area analyzer. **Figure 6** presents the nitrogen adsorption and desorption isotherms, along with the pore size distribution of ZnO hollow structures synthesized from different precursors. The nitrogen adsorption shows a type III isotherm with a hysteresis loop, indicating the presence of mesopores (2–50 nm) and macropores (> 50 nm). Adsorption for ZnO synthesized from zinc nitrate is approximately ten times higher than from zinc acetate and five times higher than from zinc chloride, suggesting more mesopores in the zinc nitrate sample, as corroborated by FE-SEM images. The BJH plot reveals a bimodal pore size distribution, with zinc acetate showing peaks at 2–4 nm (micropores), while Zinc chloride shows a pore size distribution graph with two prominent peaks in the range of 8 to 10, indicating the presence of mesoporous. The zinc nitrate sample demonstrates a wide distribution from 1 to 100 nm, with peaks at 15 and 24 nm, indicating a well-developed porous structure and significantly larger pore volumes compared to the other precursors [15,17].

Table 4 summarizes the physical parameters of the synthesized samples, showing that zinc nitrate and zinc chloride samples have higher specific surface areas and more uniform structures than those from zinc acetate. The increased porosity of ZnO hollow spheres primarily stems from their hollow morphology and the effective removal of template species during hydrothermal synthesis. Samples derived from Zinc Chloride and Zinc Nitrate exhibited a higher specific surface area and well-defined mesoporous structure compared to those synthesized from Zinc Acetate. The superior porosity of ZnO hollow spheres obtained from Zinc Chloride and Zinc Nitrate precursor can be attributed to the well-defined hollow morphology and efficient removal of template species during hydrothermal synthesis [18,19].

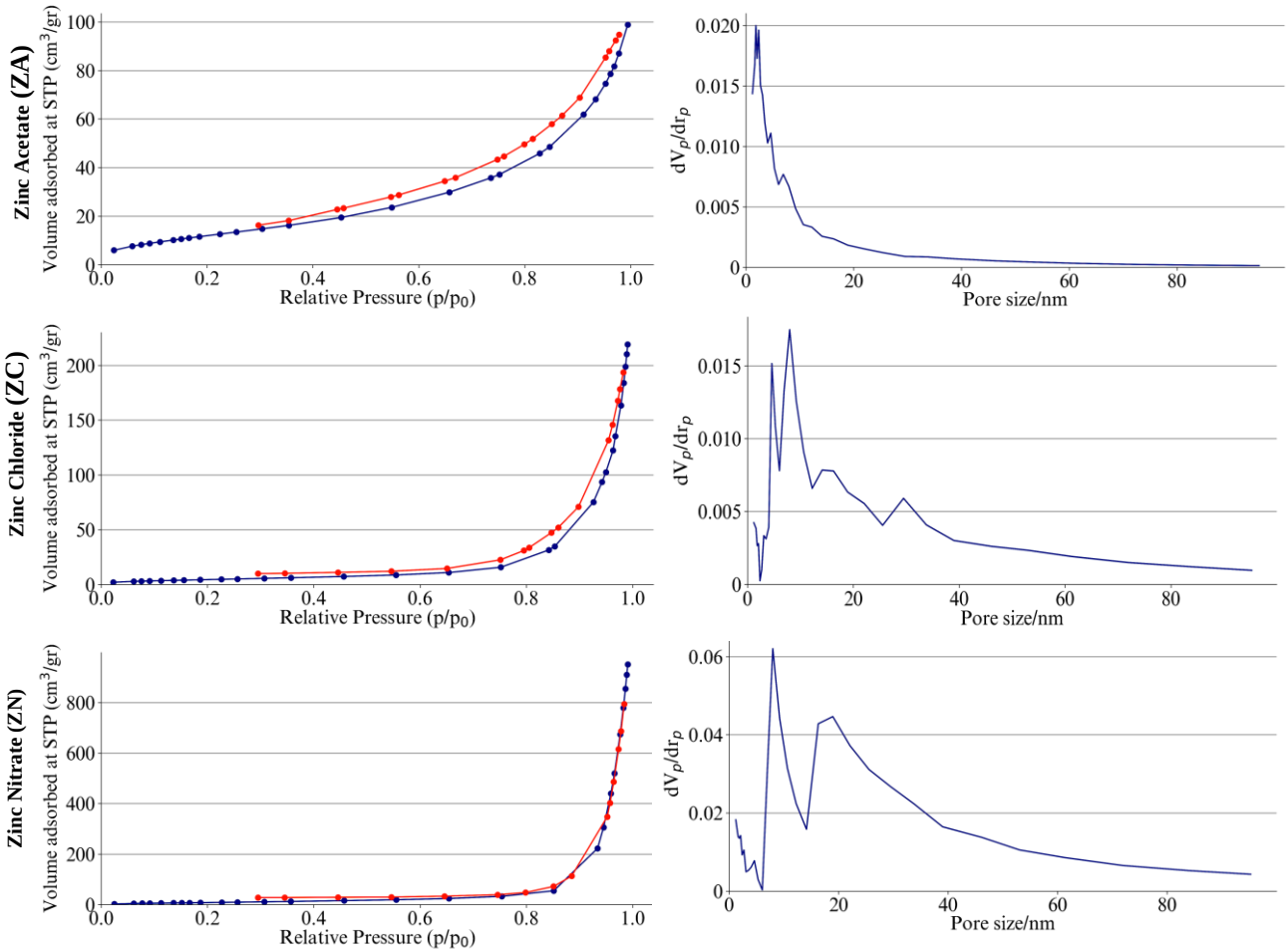

Figure 6. Nitrogen adsorption isotherm and pore size distribution curve (inset) of the samples synthesis by different precursors characterized by BET & BJH techniques.

Table 4. Specific surface area, mean pore diameter, pore volume of the sample's synthesis with different precursors.

Material	Specific surface area ($m^2 \cdot g^{-1}$)	Mean pore diameter [nm]	Pore volume ($cm^3 \cdot g^{-1}$)
Zinc Chloride (ZC)	48.829	161.75	1.445
Zinc Nitrate (ZN)	35.722	72.69	0.333
Zinc Acetate (ZA)	18.271	12.1	0.1477

4. Conclusion

Hydrothermal synthesis successfully produced ZnO hollow spheres using all three precursors (Zinc Nitrate, Zinc Acetate, and Zinc Chloride).

- Field-emission scanning electron microscopy (FE-SEM) images revealed greater uniformity in hollow spheres synthesized with Zinc Chloride and Zinc Nitrate compared to Zinc Acetate.
- Thermogravimetric analysis (TGA) analysis indicated a higher production efficiency of ZnO using the Zinc Acetate precursor. However, this method resulted in irregular and rod-shaped particles with incomplete conversion to hollow spheres.
- The thermogravimetric analysis (TGA) curve displayed two exothermic peaks around 300 ℃ and 440 ℃. These peaks likely correspond to the evaporation of

adsorbed water molecules from the ZnO surface, the removal of organic content and impurities from the lattice, and the conversion of $Zn(OH)_2$ to ZnO.

- The specific surface area, average diameter, and void volume of the hollow spheres decreased in the order of Zinc Chloride, Zinc Nitrate, and Zinc Acetate precursors.
- Notably, Zinc Nitrate and Zinc Chloride precursors yielded well-defined hollow spheres with high surface area and porosity. This makes them promising candidates for various applications requiring tailored nanostructured ZnO materials.

Author contributions: Conceptualization, OK, KN and HNS; investigation, OK; writing—review and editing, OK, KN and HNS; writing—original draft, OK; project administration, KN and HNS; funding acquisition, KN and HNS; discussion on results, KN and HNS; writing the results, KN and HNS; visualization, KN and HNS; resources, KN and HNS; data-curation, KN and HNS. All authors have read and agreed to the published version of the manuscript.

Research data policy and data availability statements: On reasonable request, the corresponding author will make available the datasets used and/or created during this investigation. The experimental work and language of the manuscript are also unique. There was no evidence of plagiarism in the submitted manuscript. If the reviewer insists on seeing the evidence, we would gladly deliver it to them in a plagiarized form. The data that support the findings of this study are available from the corresponding author upon reasonable request.

Conflict of interest: The authors declare no conflict of interest.

References

1. Yadav M, Kumar M, Chaudhary S, et al. A Review on Chemiresistive Hybrid Zinc Oxide and Nanocomposites for Gas Sensing. Industrial & Engineering Chemistry Research. 2023; 62(29): 11259–11278. doi: 10.1021/acs.iecr.3c00242
2. Krishna KG, Umadevi G, Parne S, et al. Zinc oxide based gas sensors and their derivatives: a critical review. Journal of Materials Chemistry C. 2023; 11(12): 3906–3925. doi: 10.1039/d2tc04690c
3. Qu Y, Ding Z, Yuan X, et al. Highly responsive n-butanol gas sensor based on double-shell ZnO hollow microspheres. Microchemical Journal. 2024; 200: 110242. doi: 10.1016/j.microc.2024.110242
4. Hossain MS, Furusawa T, Sato M. Sucrose-derived carbon template-assisted synthesis of zinc oxide hollow microspheres: Investigating the effect of hollow morphology on photocatalytic activity. Inorganic Chemistry Communications. 2023; 148: 110376. doi: 10.1016/j.inoche.2022.110376
5. Allag N, Bouafia A, Chemsa B, et al. Effect of precursors on structural, optical and surface properties of ZnO thin film prepared by spray pyrolysis method: efficient removal of Cu (II) from wastewater. Transition Metal Chemistry. 2023; 49(1): 39–51. doi: 10.1007/s11243-023-00560-9
6. Bahtoun H, Hadjeris L, Iaiche S, et al. Effect of ZnO Nanoparticles Salt Precursors on Structural, Morphological, Optical and MB Photocatalytic Properties Using Hydrothermal Synthesis. Journal of Nano Research. 2023; 77: 87–104. doi: 10.4028/p-82qxbi
7. Xu LL, Zhao PQ, Wu XL, et al. Synthesis of ZnO eggshell-like hollow spheres via thermal evaporation at low temperature. Journal of Physics D: Applied Physics. 2007; 40(15): 4621–4624. doi: 10.1088/0022-3727/40/15/039
8. Fang B, Zhang C, Wang G, et al. A glucose oxidase immobilization platform for glucose biosensor using ZnO hollow nanospheres. Sensors and Actuators B: Chemical. 2011; 155(1): 304–310. doi: 10.1016/j.snb.2010.12.040

9. Wang J, Luo X, Young C, et al. A Glucose-Assisted Hydrothermal Reaction for Directly Transforming Metal–Organic Frameworks into Hollow Carbonaceous Materials. Chemistry of Materials. 2018; 30(13): 4401–4408. doi: 10.1021/acs.chemmater.8b01792
10. Parvaz S, Rabbani M, Rahimi R. Fabrication of novel magnetic ZnO hollow spheres/pumice nanocomposites for photodegradation of Rhodamine B under visible light irradiation. Materials Science and Engineering: B. 2021; 263: 114863. doi: 10.1016/j.mseb.2020.114863
11. Tohidi T, Tohidi S, Mohammad-Rezaei R. Fabrication of flexible polyaniline@ZnO hollow sphere hybrid films for high-performance NH3 sensors. Journal of Materials Science: Materials in Electronics. 2020; 31(21): 19119–19129. doi: 10.1007/s10854-020-04448-7
12. Agarwal S, Kumar S, Agrawal H, et al. An efficient hydrogen gas sensor based on hierarchical Ag/ZnO hollow microstructures. Sensors and Actuators B: Chemical. 2021; 346: 130510. doi: 10.1016/j.snb.2021.130510
13. Yin M, Liu S. Preparation of ZnO hollow spheres with different surface roughness and their enhanced gas sensing property. Sensors and Actuators B: Chemical. 2014; 197: 58–65. doi: 10.1016/j.snb.2014.02.071
14. Mousavi SM, Golestaneh M. Facile Synthesis of Fe/ZnO Hollow Spheres Nanostructures by Green Approach for the Photodegradation and Removal of Organic Dye Contaminants in Water. Journal of Nanostructures. 2021; 11(1). doi: 10.22052/JNS.2021.01.003
15. Prasongsook P, Lachom V, Kenyota N, et al. Characterization and photocatalytic performance of hollow zinc oxide microspheres prepared via a template-free hydrothermal method. Materials Chemistry and Physics. 2019; 237: 121836. doi: 10.1016/j.matchemphys.2019.121836
16. Agrawal N, Munjal S, Ansari MZ, et al. Superhydrophobic palmitic acid modified ZnO nanoparticles. Ceramics International. 2017; 43(16): 14271–14276. doi: 10.1016/j.ceramint.2017.07.176
17. Ramimoghadam D, Hussein MZB, Taufiq-Yap YH. Synthesis and characterization of ZnO nanostructures using palm olein as biotemplate. Chemistry Central Journal. 2013; 7(1). doi: 10.1186/1752-153x-7-71
18. Deng Z, Chen M, Gu G, et al. A Facile Method to Fabricate ZnO Hollow Spheres and Their Photocatalytic Property. The Journal of Physical Chemistry B. 2007; 112(1): 16–22. doi: 10.1021/jp077662w
19. Wang M, Cao X, Wang L, et al. Template-free fabrication of porous zinc oxide hollow spheres and their enhanced photocatalytic performance. Journal of Porous Materials. 2009; 17(1): 79–84. doi: 10.1007/s10934-009-9266-7